

Numerical studies of heat transfer with shear thinning fluids in scraped-surface heat exchangers

D. L. Pyle (1), K.-H. Sun (2), N. Hall-Taylor (3), A. D. Fitt (4), C. P. Please (5), M. J. Baines (6)

(1) School of Food Biosciences, University of Reading, RG6 6AP, UK

d.l.pyle@reading.ac.uk

(2) School of Food Biosciences, University of Reading, RG6 6AP, UK

k.sun@reading.ac.uk

(3) Chemtech International Ltd, Reading, RG2 0LP, UK

nick@chemtechinternational.com

(4) School of Mathematics, University of Southampton, SO17 1BJ, UK

adf@maths.soton.ac.uk

(5) School of Mathematics, University of Southampton, SO17 1BJ, UK

cpp@maths.soton.ac.uk

(6) Department of Mathematics, University of Reading, RG6 6AP, UK

m.j.baines@reading.ac.uk

Abstract

Heat transfer in scraped-surface heat exchangers (SSHEs) is studied using Finite Element numerical methods for a hydrodynamic fully developed flow. The fluid is assumed to be non-Newtonian, specifically shear thinning. The results show the shear thinning index and thermal boundary conditions affect the axial local and overall heat transfer. Matters concerning scale-up problems and ideas for improving overall heat transfer performance are also discussed.

Key-words: CFD, Heat Transfer, Power Law, Viscous Dissipation.

Introduction

Scraped-surface heat exchangers (SSHEs) are a type of multifunctional food processing component. They are widely used for continuously sterilizing, cooling and texturing of highly viscous food materials such as margarine, peanut butter, salad dressing, jam, thick soups and ice-cream. Most such foodstuffs are non-Newtonian and their viscosity is highly temperature dependent. In a typical SSHE, the outer cylinder is jacketed (for heating or cooling) and blades are attached to the rotating shaft (inner cylinder). As the food material is pumped through the annular gap, the blades (scrapers) periodically remove material from the heat transfer surface to prevent fouling and increase mixing. SSHEs can therefore be used to provide the controlled (high-temperature-short-time) heat transfer that is routinely required for structuring delicate materials. A detailed understanding of SSHE operation is crucial as both the nutritional content and textural attractiveness of the final products depend critically on the mechanical and thermal histories of the material during processing. The food industry is therefore extremely interested in improving understanding of SSHEs to maximise productivity, improve product quality, whilst minimising energy consumption and improving food product novelty.

Owing to the complex geometry and typical internal environment in an SSHE, experimental studies have mainly been limited to quantifying global effects or integral values, such as energy input, residence time distribution and overall heat transfer performance [1]. Since an appreciation of the local flow behaviour is crucial for understanding the combined mechanical and thermal properties of an SSHE, extensive experimental efforts have been undertaken to study flow in model SSHE systems in the absence of heat transfer [2, 3, 4]. Numerical and analytical studies have also been carried out with non-Newtonian fluids for isothermal problems relevant to SSHEs [5, 6]. A 3D non-isothermal numerical study [7] determined the flow of a Newtonian fluid in an SSHE, predicting the velocity, temperature distribution and Nusselt number. Numerical studies of flow and heat transfer problems have also been studied [8, 9, 10] for a range of 2D and quasi-3D sub-problems in simplified SSHE geometries with power law fluids. A valuable modelling approach has been to develop models of sub- or paradigm problems of direct relevance to SSHE design and operation. The results demonstrate how the blade mounting sites and the blade hole details affect the flow, mixing and local stagnation zones. The results also show the effects of fluid shear- and heat-thinning on the size of the local viscous dissipation. In particular, it is clear that in high shear regions the local viscous heating is much smaller and heat thinning effects are thus reduced for shear thinning fluids compared to Newtonian fluids.

In this study, we examine the effects of axial flow on the flow and heat transfer for a fully developed (large Prandtl number) power law fluid hydrodynamic flow. The results show the effects of the shear

thinning index and thermal boundary conditions on both local axial and overall heat transfer. Scale-up problems and possibilities for improving overall heat transfer performance are also discussed.

Differential equations and numerical procedure

In a typical SSHE, the outer cylinder of radius R, say, is stationary. The blades are attached to an inner cylinder (radius L) that rotates at a constant speed U. We consider SSHE flow in a rectangular coordinate system with the frame of reference fixed in the inner cylinder i.e. rotating at constant angular velocity $\omega=U/L$. The x- and y-axes are in the plane of the tangential flow and the z-axis is in the direction of the axial flow. A schematic view of a cross section at an x-y plane, the blade mounting positions and the coordinate system is given in Fig. 1, which shows the outer cylinder rotating in a clockwise direction. In the configuration considered here, the radius ratio is $RR=1.5$ and four blades (without leakage) are evenly spaced around the cylinder circumference and mounted tangentially to the inner cylinder.

If the physical properties of the fluids (density, viscosity, specific heat, thermal conductivity etc.) are assumed independent of temperature and there is no phase change during device operation, then the velocity de-couples from the temperature. Owing to the high viscosity of typical SSHE fluids the Prandtl number is very large (>1000). Thermal boundary layers are therefore much thinner than velocity boundary layers. We assume that the velocity profile is fully developed before the fluid enters the heating zone. Thus the velocity does not change with either axial location or the thermal boundary conditions and may be determined first. The temperature is then determined separately using the known velocity field.

Flow equations and boundary conditions

We consider isothermal, laminar, steady flow of an incompressible viscous fluid. It is reasonable to assume that all the velocity components are functions of x and y only, and, from the w momentum equation, the axial pressure gradient is therefore also independent of z. The flow field is the same at any cross section in x-y plane. The velocity scales are the inner cylinder velocity U for the tangential velocity components u and v, and the average axial velocity W for the axial velocity component w. The scales for length and pressure are the inner cylinder radius L and $\mu_F U/L$, respectively. The

characteristic viscosity μ_F is the viscosity given at a shear rate $\dot{\gamma} = \left((U/L)^2 + (W/L)^2 \right)^{1/2}$. Neglecting Coriolis forces, at any cross section in the x-y plane the non-dimensional governing equations are

$$\frac{\partial u^*}{\partial x^*} + \frac{\partial v^*}{\partial y^*} = 0 \quad (1)$$

$$Re_U \left(u^* \frac{\partial u^*}{\partial x^*} + v^* \frac{\partial u^*}{\partial y^*} \right) = -\frac{\partial p^*}{\partial x^*} + \frac{\partial}{\partial x^*} \left(\frac{\mu}{\mu_F} \frac{\partial u^*}{\partial x^*} \right) + \frac{\partial}{\partial y^*} \left(\frac{\mu}{\mu_F} \frac{\partial u^*}{\partial y^*} \right) \quad (2)$$

$$Re_U \left(u^* \frac{\partial v^*}{\partial x^*} + v^* \frac{\partial v^*}{\partial y^*} \right) = -\frac{\partial p^*}{\partial y^*} + \frac{\partial}{\partial x^*} \left(\frac{\mu}{\mu_F} \frac{\partial v^*}{\partial x^*} \right) + \frac{\partial}{\partial y^*} \left(\frac{\mu}{\mu_F} \frac{\partial v^*}{\partial y^*} \right) \quad (3)$$

$$Re_U \left(u^* \frac{\partial w^*}{\partial x^*} + v^* \frac{\partial w^*}{\partial y^*} \right) = f Re_W + \frac{\partial}{\partial x^*} \left(\frac{\mu}{\mu_F} \frac{\partial w^*}{\partial x^*} \right) + \frac{\partial}{\partial y^*} \left(\frac{\mu}{\mu_F} \frac{\partial w^*}{\partial y^*} \right) \quad (4)$$

where * denotes a non-dimensional variable, $Re_U = \rho UL / \mu_F$ is the tangential Reynolds number,

$Re_W = \frac{\rho WL}{\mu_F}$ is the axial flow Reynolds number, or a non-dimensional axial volume flux, and $f = \frac{-p_z L}{\rho W^2}$

is the non-dimensional axial pressure gradient or friction factor. The frictional pressure gradient is

$$\text{defined as } f \cdot Re_W = \frac{-p_z L}{\rho W^2} \cdot \frac{\rho WL}{\mu_F} = \frac{-p_z L^2}{\mu_F W}.$$

The velocity ratio or Reynolds number ratio is $\alpha = \frac{W}{U} = \frac{Re_W}{Re_U}$. Since during industrial SSHE applications the tangential flow dominates, values of the velocity ratio are selected to be less than 0.2.

The boundary conditions in the plane of the tangential flow are

$$\text{(At the outer cylinder)} \quad u^* = RR \cos \theta, v^* = RR \sin \theta, w^* = 0. \quad (5)$$

$$\text{(At the inner cylinder and blades)} \quad u^* = v^* = w^* = 0. \quad (6)$$

A generalized shear thinning power law viscosity $\mu = c_m I_2^{(m-1)/2}$ is used. Here c_m is the consistency index (Pa-s^m), which varies with the material. The shear-thinning index m also varies with the material. A typical value of m for food materials such as fruit jam, peanut butter etc. is 0.33. Newtonian fluids are also considered in this text for completeness. I_2 is the second invariant of the shear rate tensor.

Non-dimensionalized by the characteristic viscosity $\mu_F = c_m \left(\left(\frac{U}{L} \right)^2 + \left(\frac{W}{L} \right)^2 \right)^{(m-1)/2}$ the final form of the viscosity is

$$\frac{\mu}{\mu_F} = \left(\frac{I_2^*}{(1 + \alpha^2)} + c_1 \right)^{(m-1)/2} + c_2 \quad (7)$$

$$\text{where } I_2^* = \left(2 \left(\frac{\partial u^*}{\partial x^*} \right)^2 + 2 \left(\frac{\partial v^*}{\partial y^*} \right)^2 + \left(\frac{\partial u^*}{\partial y^*} + \frac{\partial v^*}{\partial x^*} \right)^2 + \alpha^2 \left(\frac{\partial w^*}{\partial x^*} \right)^2 + \alpha^2 \left(\frac{\partial w^*}{\partial y^*} \right)^2 \right).$$

The constants c_1 and c_2 are included to ensure that the viscosity has a nonzero finite value in the whole domain. Values of $c_1=0.000001$ and $c_2=0.0001$ were selected; numerical experiments show that this modification has an insignificant effect on the bulk viscosity whilst giving physically reasonable viscosity values.

Energy equation and thermal boundary conditions

We assume that the entering stream has a uniform temperature T_{in} and the temperature of the outer cylinder is maintained at a constant temperature T_w , the other walls are adiabatic and the axial conduction term may be neglected. The non-dimensional temperature is $T^* = \frac{(T - T_{in})}{\Delta T}$ where the temperature difference is defined as $\Delta T = |T_{in} - T_w|$. (The absolute value is used so that the Brinkman number is positive for both cooling and heating.) The energy equation is

$$Pe_U \left(u^* \frac{\partial T^*}{\partial x^*} + v^* \frac{\partial T^*}{\partial y^*} \right) + Pe_W w^* \frac{\partial T^*}{\partial z^*} = \frac{\partial^2 T^*}{\partial x^{*2}} + \frac{\partial^2 T^*}{\partial y^{*2}} + Br \left(\frac{\mu}{\mu_F} \right) I_2^* \quad (8)$$

where $Pe_U = Pr \cdot Re_U$ and $Pe_W = Pr \cdot Re_W$ are the Peclet numbers corresponding to the tangential and axial flows, respectively. The Prandtl number is $Pr = \frac{c_p \mu_F}{k}$ and the Brinkman number is $Br = \frac{\mu_F U^2}{k \Delta T}$.

The thermal boundary conditions in the plane of the tangential flow are

$$\text{(At the outer cylinder): Isothermal, } T_w^* = \pm 1, \text{ heating / cooling.} \quad (9)$$

$$\text{(At the inner cylinder and the blades): Adiabatic, } \frac{dT^*}{dn^*} = 0. \quad (10)$$

$$\text{The initial temperature at the inlet } z^*=0 \text{ is assumed to be } T_{in}^* = 0. \quad (11)$$

At a given axial location, the heat transfer between the outer cylinder and the fluid is characterised by the wall heat flux and bulk-mean temperature. The axial local wall heat flux at a location z is defined

as $q = -k \frac{\partial T}{\partial n} \Big|_{R,z}$. The fluid bulk-mean temperature is an axial/longitudinal flow-weighted average of

the local fluid temperature $T_m = \frac{\int_A wT dA}{\int_A w dA}$. In this text the term “wall heat flux” refers to the

dimensionless circumferentially-averaged axial local wall heat flux given by $Nu = q^* = \frac{qL}{k\Delta T} = -\frac{1}{2\pi RR} \int_{RR} \frac{\partial T^*}{\partial n^*} \Big|_{z^*}$ which will be positive for cooling and negative for heating conditions.

The non-dimensional partial differential equations above were solved using with the commercial finite element partial differential equation solver FastfloTM [11]. This is not a “black box” CFD package. Selected numerical methods have to be implemented through user programming. To solve for the flow field, the augmented Lagrangian method and Newton-Raphson method were used. Knowing the velocity, the energy equation may be solved by a marching scheme in the axial direction. The basic computer code implemented here is the same as that used for previous cases ([8, 9, 10]) where a detailed discussion of the mesh, numerical formulation for the velocity and temperature fields may be found.

Results and discussions

For power law fluids, the non-dimensional parameters are interdependent. For instance, if the cylinder rotation velocity changes then the Reynolds number, Peclet number and Brinkman number will also change. Therefore parametric studies need to be carried out in two different ways. One is to change individual non-dimensional parameters. For scale-up purposes, individual physical parameters are changed. For the computations recorded here, the values $L=0.05\text{m}$ and $W=0.1\text{m/s}$ were used. The dimensionless pressure, tangential flow quasi-streamlines and axial velocity at a cross section of a SSHE for $m=0.33$, $Re_U = 3.17$ ($U=0.5\text{m/s}$) are shown in Fig. 1. The corresponding dimensionless temperature fields for cooling with $Pe_w=2000$, $Br=0.164$ at $z=0.1, 0.2, 1.0$ and 1.8m are shown in Fig. 2. On the temperature contour plots, lower contour values are represented by a darker colour. Near the entrance the temperature is uniform ($z=0.1\text{m}$), and further down the channel the cooling effect can be seen.

Fig. 3 shows the axial local averaged heat flux and bulk-mean temperature for heating and cooling at $Br=0.41667$, $Re_U=10$, $Pe_w=500$, $m=0.33$ ($U=1\text{m/s}$). Note that the Reynolds number does not vary linearly with U because of the change in characteristic viscosity. Due to viscous dissipation, extra heat needs to be removed from the wall for cooling of the fluid material while less heat is required for heating for the same change in bulk temperature. Eventually the wall heat flux reaches the same value in a thermally fully developed region. The effects of shear thinning index on the wall heat flux and fluid bulk-mean temperature for cooling at $Br=0.41667$, $Re_U = 10$, $Pe_w=500$ ($U=1\text{m/s}$) are shown in Fig. 4. It is seen that the bulk-mean temperature is lower for $m=0.33$ than $m=1.0$. Apart from close to the entrance, the same trend is found in Nu . The reason is that the viscous dissipation is determined by local velocity gradients and the local effective viscosity. In SSHEs, close to the singularity corners the velocity gradients are very high. Therefore, the viscous dissipation is very high for constant viscosity Newtonian fluids. However, for shear thinning fluids the viscosity is reduced in high shear regions and the combined effects of high shear and low viscosity result in lower viscous dissipation. This is consistent with our 2D heat transfer results [8]. Harrod [1] also indicated that the measured heat transfer was different for heating and cooling conditions and that the largest differences were found when the materials were Newtonian. It is not surprising that similar results were found in a single screw extruder by Karwe and Jaluria [12], where the geometry is similar.

Fig. 5a shows the effect of the parameter Pe_w on the wall heat flux for cooling conditions at $Re_U=10$, $Br=0.41667$, $m=0.33$. It is seen that in SSHEs with axial flow, the wall heat flux changes with Peclet number in both the thermal entrance and thermally developed regions. This contrasts with the 2D results where there is no net contribution to the average wall flux from the convection term [8]. The effect of cylinder rotation velocity U on heat transfer for $m=0.33$ is shown in Fig. 5b. For $U=1.0\text{m/s}$ the values of the dimensionless parameters were $Re=10$, $Pe_w=2000$, $Br=0.41667$.

Conclusions

Finite element methods have been used successfully to study heat transfer in hydrodynamically fully developed flows of power law fluids in SSHEs with axial through-flow. The results show that for power law fluids the viscous dissipation is lower than for Newtonian fluids. For the same set of non-dimensional parameters, the bulk-mean temperature and wall heat flux is lower for power law fluids than for Newtonian fluids. This is consistent with our 2D SSHE results.

In SSHEs with fully developed hydrodynamic flow, the axial local averaged heat flux in the thermal entrance region and in the fully developed thermal region depends on the Peclet number.

It is seen that the wall heat flux is gradually reduced down the channel. The heat transfer could thus be improved by avoiding thermally developed regions, reducing the section length for isothermal wall temperature or by using staggered short blades.

Acknowledgements

The second author acknowledges financial support from The University of Reading.

References

1. Harrod, M. Scraped surface heat exchangers-A literature survey of flow patterns mixing effects, residence time distribution, heat transfer and power requirements. *J. Food Proc. Eng.*, 9, 1-62, 1986.
2. Wang, W., Walton, J.H., McCarthy, K.L. Flow profiles of power law fluids in scraped surface heat exchanger geometry using MRI. *J. Food Proc. Eng.*, 22, 11-27, 1999.
3. Dumont, E., Fayolle, F. and Legrand, J. Flow regimes and wall shear rates determination within a scraped surface heat exchanger. *J. Food Eng.*, 45, 195-207, 2000.
4. Rodruiguez, S. Flow measurements in scraped surface heat exchangers, PhD, Birmingham University, 2000.
5. Stranzinger M. Feigl K. and Windhab E. Non-Newtonian flow behaviour in narrow annular gap reactors. *Chem. Eng. Sci.*, 56, 3347-3363, 2001.
6. Fitt A.D. and Please C.P. Asymptotic analysis of the flow of shear-thinning food stuffs in annular scraped heat exchangers. *J. Eng. Math.*, 39, 345-366, 2001.
7. Baccar, M. and Abid, M.S. Numerical analysis of three-dimensional flow and thermal behaviour in a scraped surface heat exchanger. *Rev. Gen. Therm. Fr.*, 36, 782-790, 1997.
8. Sun, K.-H., Pyle, D.L., Fitt, A.D., Please, C.P., Baines, M.J. and Hall-Taylor, N. Numerical Study of 2D Heat Transfer in a Scraped Surface Heat Exchanger. *Int. J. Computers and Fluids*. 2003 (Accepted for publication).
9. Sun, K.-H., Pyle, D.L., Hall-Taylor, N., Baines, M.J. and Fitt, A.D. Velocity profiles and frictional pressure drop for shear thinning materials in lid driven cavities with fully developed axial flow. Submitted to *Chem. Eng. Sci.*, 2003.
10. Sun, K.-H., Pyle, D.L., Fitt, A.D., Please, C.P., Hall-Taylor, N. and Baines, M.J. Heat transfer and thermal entrance length with shear thinning materials in lid driven cavities with fully developed axial flow. 2003 (Submitted to *Int. J. Heat and Mass Transfer*).
11. *Fastflo Tutorial Guide V3*, Oxford, Numerical Algorithms Group, 2000.
12. Karwe M.V. and Jaluria Y. Numerical simulation of fluid flow and heat transfer in a single screw extruder for non-Newtonian fluids. *Numerical heat transfer A*, 17, 167-190, 1990.

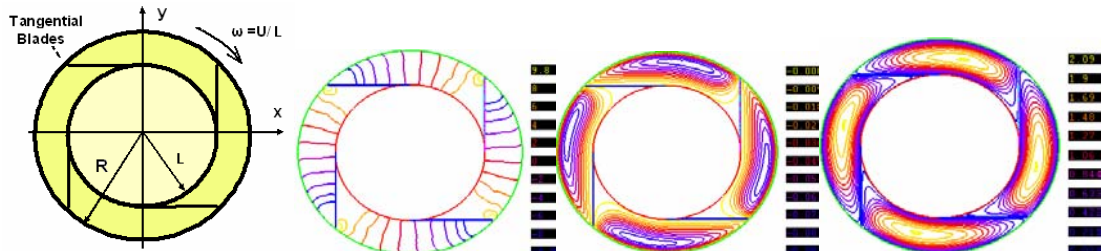


Fig.1. Schematic view of a cross section at x-y plane, pressure, quasi-streamline and axial velocity distribution for $m=0.33$, $Re_U = 3.17$.

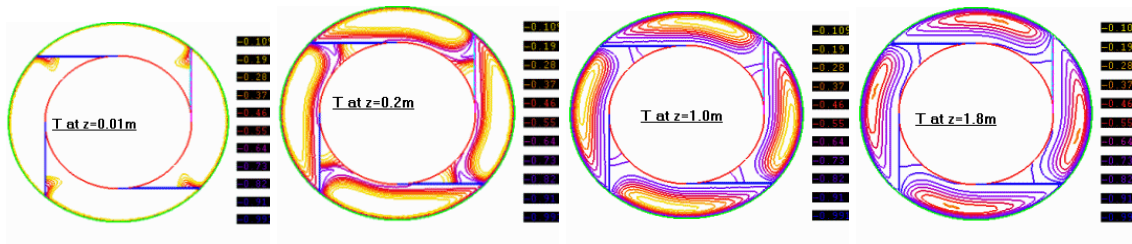


Fig. 2. Temperature distributions. Cooling for $m=0.33$, $Re_U = 3.17$, $Pew=2000$, $Br=0.164$.

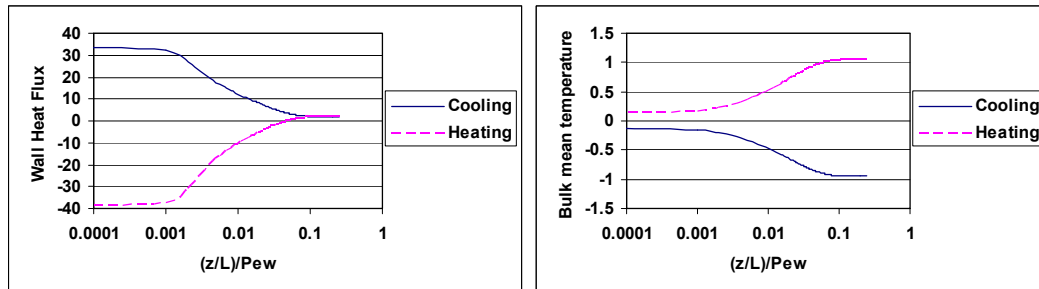


Fig. 3. Wall heat flux and fluid bulk-mean temperature for heating and cooling. $m=0.33$, $Re_U = 10$, $Pew=500$, $Br=0.41667$.

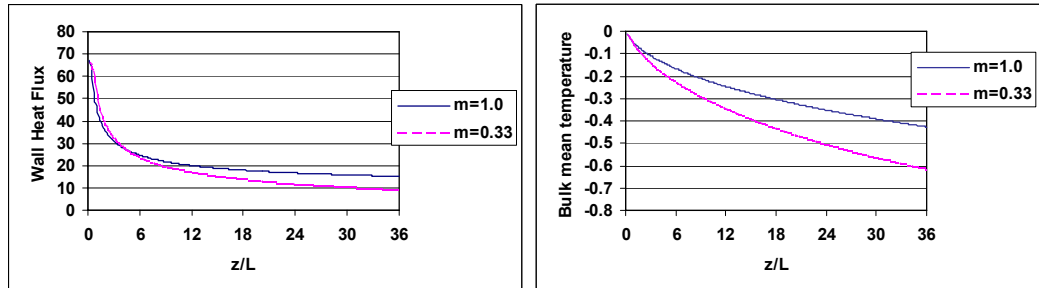


Fig. 4. Effect of m on wall heat flux and fluid bulk-mean temperature. Cooling for $Re_U = 10$, $Pew=2000$, $Br=0.41667$.

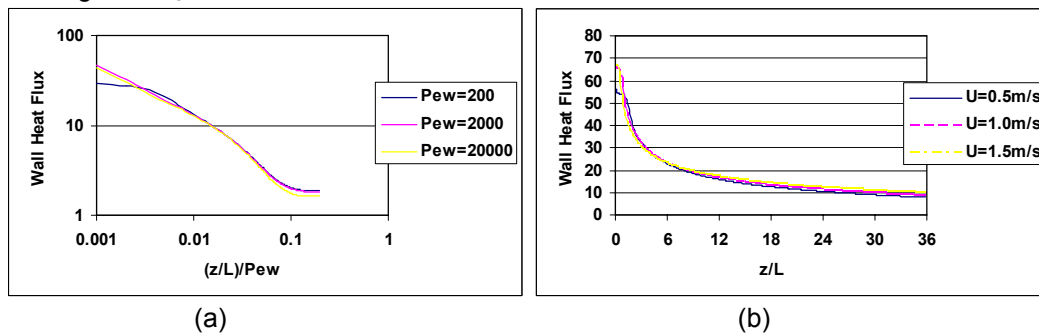


Fig. 5. a. Effect of Peclet number on heat transfer for $m=0.33$, $Re_U = 10$, $Br=0.41667$
b. Effect of rotation velocity on heat transfer for $m=0.33$.